A Comparative Investigation of Structure and Bonding in Mo and W $[TeM_6O_{24}]^{6-}$ and $[PM_{12}O_{40}]^{3-}$ Heteropolyanions

Adam J. Bridgeman*,† and Germán Cavigliasso†,‡

Department of Chemistry, University of Hull, Kingston upon Hull HU6 7RX, U.K., and Department of Chemistry, University of Cambridge, Lensfield Road, Cambridge CB2 1EW, U.K.

Received: May 15, 2003

The structure and bonding in $[TeM_6O_{24}]^{6-}$ (Anderson) and $[PM_{12}O_{40}]^{3-}$ (α-Keggin) heteropolyanions have been investigated by density-functional methods. Various molecular-orbital and population approaches have been employed in the analysis of the structural and electronic properties. Good agreement between computational and experimental or bond-valence results for bond parameters has been obtained. The M−O interactions have been found to be largely of M*d*−O*p* character, whereas the orbital nature of Te−O and P−O bonding can be predominantly characterized as Te*sp* or P*sp* and O*sp*. The interactions between the $[TeO_6]$ or $[PO_4]$ fragments and the $[M_pO_q]$ cages have been explored by a decomposition approach to the polyanion structure. The results obtained have suggested that the molecular-orbital structure of the Te−O and P−O bonds is not significantly different in the presence or absence of the metal−oxygen cages but that there is nonetheless some covalent character in the bonding of the $[TeO_6]$ and $[PO_4]$ fragments to the surrounding clusters.

Introduction

Polyoxoanion chemistry constitutes an extremely rich and active field of experimental research,[1−4] and to a large extent, this is due to the remarkable structural diversity and the wide variety of chemical and physical properties, and related applications to areas such as medicine, catalysis, solid-state technology, and chemical analysis, displayed by the heteropoly species formed by Mo and W.[4]

The structures of heteropolyoxometalates can be described by the general chemical formula $[X_nM_pO_q]^{z-}$, where M is most commonly Mo or W, and X is a main-group or transition-metal heteroatom. These structures can be characterized as an assemblage of $[XO_m]$ and $[MO_n]$ coordination polyhedra, the octahedron being the most typically observed constituent unit of the $[Mo_pO_q]$ and $[W_pO_q]$ cages.[1]

The vast majority of polyoxoanion structures (based on $[MO_6]$ units) contain no more than two unshared O atoms in each polyhedral unit, and are thus classified as type-I, if there is one terminal M−O bond, or as type-II, if two such bonds are present in a cis spatial arrangement.[1,2] Heteropoly species representative of these two categories are the Keggin $[XM_{12}O_{40}]^{z-}$ (type-I) and Anderson $[XM_6O_{24}]^{z-}$ (type-II) clusters.

Poblet and co-workers[5,6] have recently reported an extensive and detailed computational study of Keggin anions containing both main-group and transition-metal atoms. Considerable attention has been focused on the electronic configuration and magnetic properties of the Co and Fe systems[5] and also on the relative stability of the α and *β* forms of several main-group systems.[6] The analysis of other aspects of the electronic structures, for example the molecular-orbital and population properties of X−O and M−O interactions, has been somewhat more limited.

We have recently investigated (using density-functional theory) many isopolyanion systems, including $[W_4O_{16}]^{8-}$,[7,8] $[M_6O_{19}]^{z-}$,[9] $[M_7O_{24}]^{6-}$,[10] $[Mo_8O_{26}]^{4-}$,[11] and $[W_{10}O_{32}]^{z-}$.[12] The analysis of the structure and bonding in these species has been performed by application of a number of approaches, such as molecular-orbital theory, population methods, and fragment decomposition. The purpose of the present work is to extend our computational investigations to the $[TeM_6O_{24}]^{6-}$ (Anderson) and $[PM_{12}O_{40}]^{3-}$ (α-Keggin) clusters. To the best of our knowledge, no high-level calculations on this Anderson anion have been carried out, and detailed molecular-orbital and Mulliken−Mayer descriptions of this α-Keggin anion have not been reported.

Computational Approach

All density-functional calculations reported in this work were performed with the ADF (2000.02)[13−17] program. Functionals based on the Vosko−Wilk−Nusair (VWN)[18] form of the local density approximation (LDA),[19] and on a combination (labeled BP86) of Becke's 1988 exchange[20] and Perdew's 1986 correlation[21] corrections to the LDA were employed, and Slater-type-orbital (STO) basis sets of triple-ζ quality incorporating frozen cores and the ZORA relativistic approach (ADF O.1s, P.2p, Mo.3d, W.4f type-IV, ADF Te.4p type-V)[17] were utilized.

The functional and basis-set choices were based on the results of tests performed on several $[MO_4]$ and $[M_2O_7]$ species.[22,23] Geometry optimizations were carried out using LDA methods, and data on thermochemistry and energetics were extracted from single-point BP86 calculations. Bond and valency indexes were obtained according to the definitions proposed by Mayer[24,25] and by Evarestov and Veryazov,[26] with a program[27] designed

* To whom correspondence should be addressed. Phone: +44 1482 466549. Fax: +44 1482 466410. E-mail: A. J.Bridgeman@hull.ac.uk.
† University of Hull.
‡ University of Cambridge.

10.1021/jp0353441 CCC: $25.00
Published on Web 08/05/2003

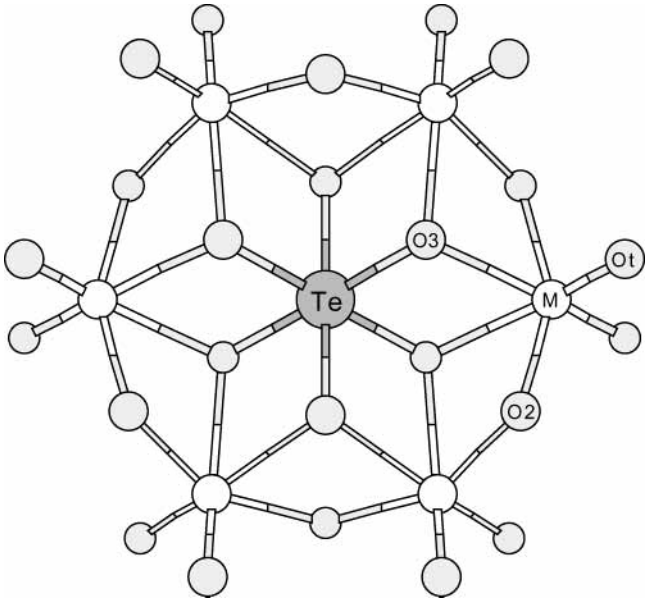

Figure 1. Structural and atom-labeling schemes for $[TeM_6O_{24}]^{6-}$ anions.

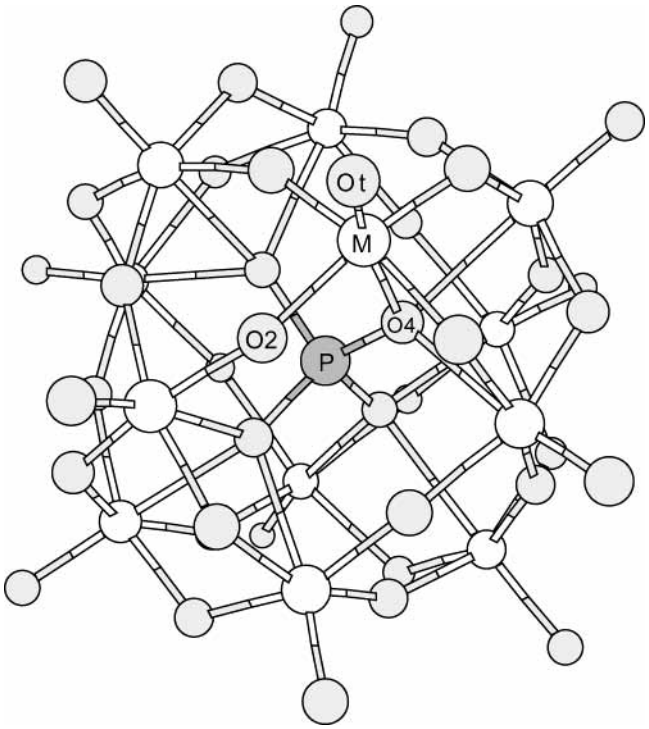

Figure 2. Structural and atom-labeling schemes for $[PM_{12}O_{40}]^{3-}$ anions.

for their calculation from the ADF output file. Graphics of molecular orbitals were generated with the MOLEKEL[28] program.

Results and Discussion

Molecular Structures. Structural schemes for the Anderson and α-Keggin anions are presented in Figures 1 and 2, respectively. Optimized bond distances for the particular species investigated are given in Table 1 and are compared with experimental data obtained from studies of crystalline phases of $[TeM_6O_{24}]^{6-}$ [29,30] and $[PM_{12}O_{40}]^{3-}$.[31−33]

The Anderson structure is closely related to that of the α isomer of $[Mo_8O_{26}]^{4-}$.[11] It possesses ideal D_{3d} symmetry and contains a "ring" of six (distorted) octahedra in which the metal atoms are interconnected via M−O−M bridges provided by the two-coordinate (O_{2c}, O2) and three-coordinate (O_{3c}, O3) oxygen sites. There are two terminal ($M-O_t$) bonds per metal center (a type-II polyanion characteristic), and the central heteroatom (Te) is bonded to all six O_{3c} atoms in a regular octahedral arrangement.

The α-Keggin structure exhibits ideal T_d symmetry, and as in the Anderson anions, the metal centers are all equivalent and three groups of oxygen sites are observed, these being terminal (O_t), two-coordinate (O_{2c}, O2), and four-coordinate (O_{4c}, O4) atoms. However, unlike the Anderson systems, there is one metal−oxygen terminal bond in each octahedral unit (a type-I polyanion characteristic), and the central heteroatom (P) lies in a regular tetrahedral environment created by the four O_{4c} atoms.

The calculated bond lengths of the $[TeM_6O_{24}]^{6-}$ and $[PM_{12}O_{40}]^{3-}$ clusters compare reasonably well with experimental data. The best agreement is found for bridging M−O bonds, especially for those involving two-coordinate oxygen sites, and the most noticeable deviations occur in terminal and heteroatom bonds.

Electronic Structure. Eigenvalue diagrams for the $[TeM_6O_{24}]^{6-}$ and $[PM_{12}O_{40}]^{3-}$ anions are shown in Figures 3 and 4, and qualitative molecular-orbital schemes, containing predominant oxygen, metal, and heteroatom contributions to the valence levels of the clusters are presented in Figures 5−8. In addition to the polyanions, the qualitative schemes include a separate analysis of the bonding between the heteroatom and its nearest coordination environment, which is carried out via the use of model $[TeO_6]^{6-}$ and $[PO_4]^{3-}$ species.

TABLE 1: Optimized X−O and M−O Distances (in pm) for $[TeM_6O_{24}]^{6-}$ and $[PM_{12}O_{40}]^{3-}$ Anions[a]

	molecule	
parameter	$[TeMo_6O_{24}]^{6-}$	$[TeW_6O_{24}]^{6-}$
Te−O	199 (193)	198 (193)
$M-O_t$	176 (172)	176 (173)
$M-O_{2c}$	194 (194)	194 (193)
$M-O_{3c}$	227 (228)	231 (228)
parameter	$[PMo_{12}O_{40}]^{3-}$	$[PW_{12}O_{40}]^{3-}$
P−O	157 (153)	157 (153)
$M-O_t$	171 (167)	173 (170)
$M-O_{2c}$	191 (192)	192 (191)
$M-O_{4c}$	241 (243)	244 (244)

[a] Experimental results are given in parentheses.

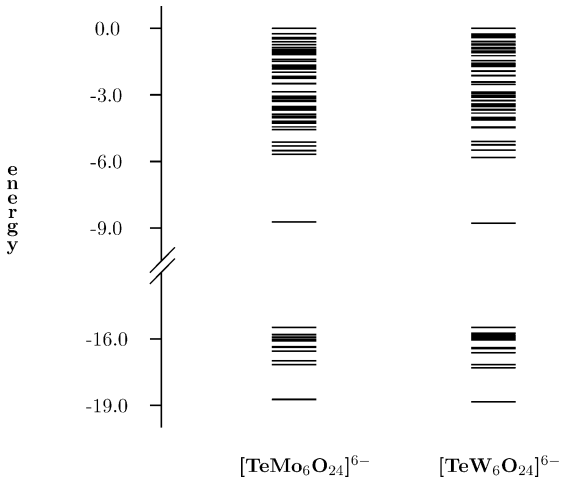

Figure 3. Eigenvalue (in eV) diagram for occupied valence levels of $[TeM_6O_{24}]^{6-}$ anions. The highest-occupied level is used as reference.

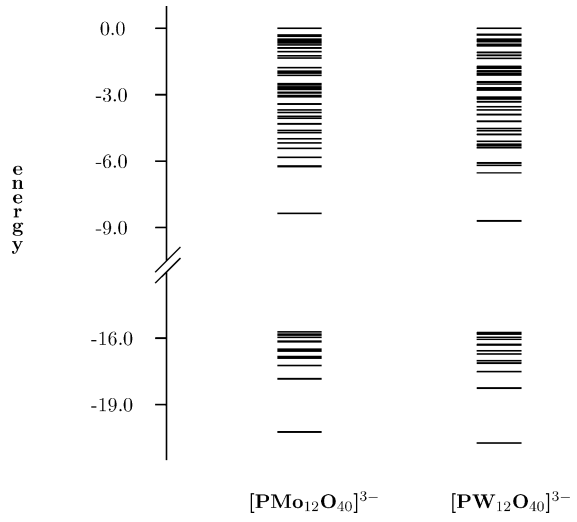

Figure 4. Eigenvalue (in eV) diagram for occupied valence levels of $[PM_{12}O_{40}]^{3-}$ anions. The highest-occupied level is used as reference.

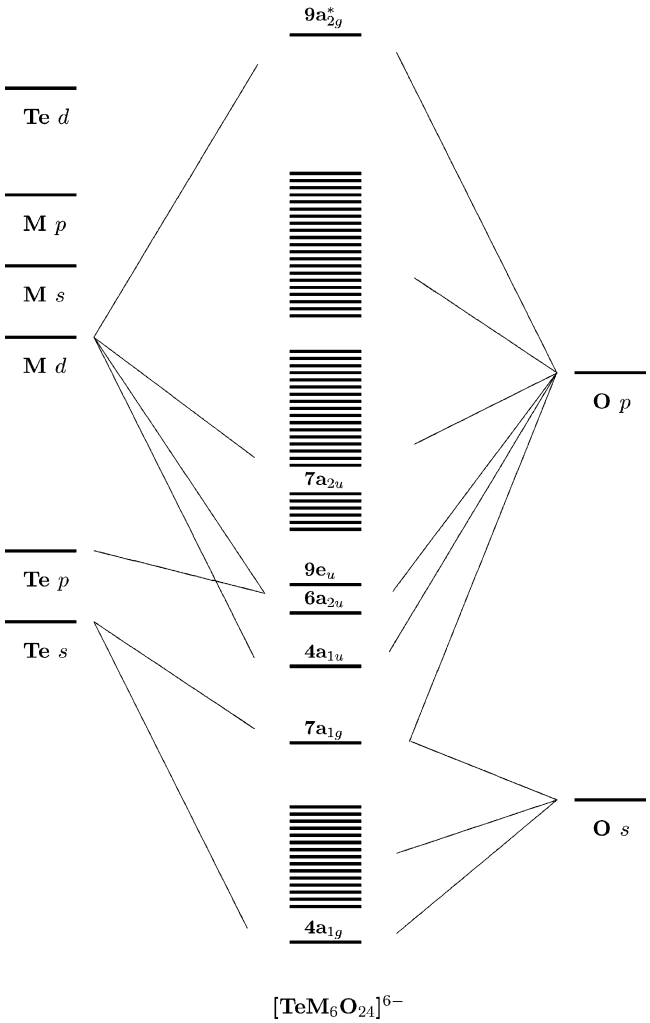

Figure 5. Qualitative molecular-orbital diagram showing predominant Te, M, and O contributions to the valence levels of $[TeM_6O_{24}]^{6-}$ anions.

It should be noted that the schemes in Figures 5−8 are entirely qualitative, and no accurate quantitative correlation exists among the positions of the atomic and molecular energy levels. These schemes are intended to summarize the most general and representative characteristics of the electronic structure of the polyanions by highlighting the major atomic contributions to the molecular orbitals.

Molecular-Orbital Diagrams. The quantitative and qualitative features of the molecular-orbital diagrams of $[TeM_6O_{24}]^{6-}$ and $[PM_{12}O_{40}]^{3-}$ anions are, in general, similar to those characteristic of the isopolyanions considered in previous publications. However, there are also some important differences because of the presence of the heteroatom.

A separation of the energy levels into two sets is observed, with the gap being approximately 10 eV and the lower and upper sets corresponding, respectively, to orbitals based on O*s* and O*p* functions. There is an additional level associated with the heteroatom that lies between these two sets (approximately 7 eV higher than the O*s* band). This level corresponds to the $7a_{1g}$ and $8a_1$ orbitals in $[TeM_6O_{24}]^{6-}$ and $[PM_{12}O_{40}]^{3-}$, respectively.

The bonding between the Mo or W sites and the O atoms arises predominantly from interactions of M*d*-type functions with O*p*-type functions, the contributions from O*s*, M*s*, and M*p* orbitals being minor or not significant. The O*p* orbitals are also involved in a largely nonbonding band that comprises the majority of the high-lying levels, and in the type-I α-Keggin systems—as in the $[M_6O_{19}]^{2-}$ and $[W_{10}O_{32}]^{4-}$ isopoly clusters[9,12]—is "split" by a M−O bonding ($17t_1$) level that lies appreciably higher in energy than the rest of the M*d*−O*p* band.

The Te−O_{3c} and P−O_{4c} bonds in $[TeM_6O_{24}]^{6-}$ and $[PM_{12}O_{40}]^{3-}$ can be described in terms of three groups of molecular orbitals, these interactions being predominantly of X*s*−O*s* ($4a_{1g}$, $4a_1$), X*s*−O*sp* ($7a_{1g}$, $8a_1$), and X*p*−O*p* ($6a_{2u} + 9e_u$, $15t_2$) character. This molecular-orbital structure of the bonding to the heteroatom is, in general, mostly unaffected by the interactions between the central $[TeO_6]$ and $[PO_4]$ fragments and the rest of the metal−oxygen cage, as observed in the diagrams of Figures 6 and 8. (It should be noted that the $[TeO_6]^{6-}$ model possesses O_h symmetry.)

Metal−Oxygen Closed Loops. Nomiya and Miwa [34] have considered that delocalized σ and π bonding along the interpenetrating M−O closed loops observed in polyanions should behave as a structural-stability factor. This idea has been quantified in the form of an index (η) defined as

$$\eta = \frac{\sum BC}{A} \qquad (1)$$

where A is the number of octahedra constituting the polyanion cage, B is the number of MO_6 units constituting the closed loop, and C is the number of closed loops. (It should be noted that the polyanion cage is not necessarily identical with the whole structure, although it does comprise most of it.[34]) Also, it has been suggested that structures with a higher η value should be more stable, but sometimes additional factors have been invoked in cases where this idea does not seem to work.[34−38]

Nomiya and Miwa [34] have proposed $[M_6O_6]$ closed loops for both the Anderson and the α-Keggin structures. In $[TeM_6O_{24}]^{6-}$, these closed loops are equivalent to those observed in the α isomer of $[Mo_8O_{26}]^{4-}$,[11] and involve all of the metal sites and all of the two-coordinate oxygen atoms. Spatial plots of the $4a_{1u}$ and $7a_{2u}$ orbitals that correspond to rings with σ and π properties, respectively, are given in Figure 9.

In the $[PM_{12}O_{40}]^{3-}$ anions, four equivalent $[M_6O_6]$ rings can be generated through the interactions between the metal and two-coordinate oxygen atoms. The diagram of Figure 7 includes all of the levels (represented by the $2a_2$, $9t_1$, $10t_1$, $9a_1$, $18t_2$, 13e, $17t_1$ set) in which the O contributions are almost exclusively from O_{2c} sites. The $2a_2$ (σ-like) and the $9a_1$ (π-like) orbitals are plotted in Figures 10 and 11, respectively. These orbitals involve all 12 M and all 24 O_{2c} atoms and, therefore, contain the four possible $[M_6O_6]$ closed loops.

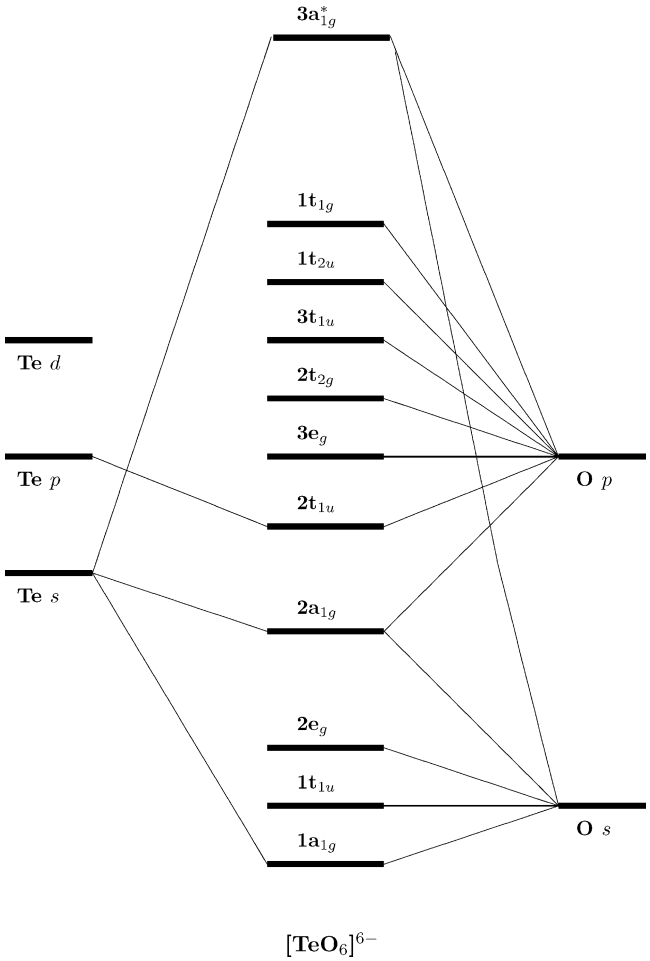

Figure 6. Qualitative molecular-orbital diagram showing predominant Te and O contributions to the valence levels of $[TeO_6]^{6-}$.

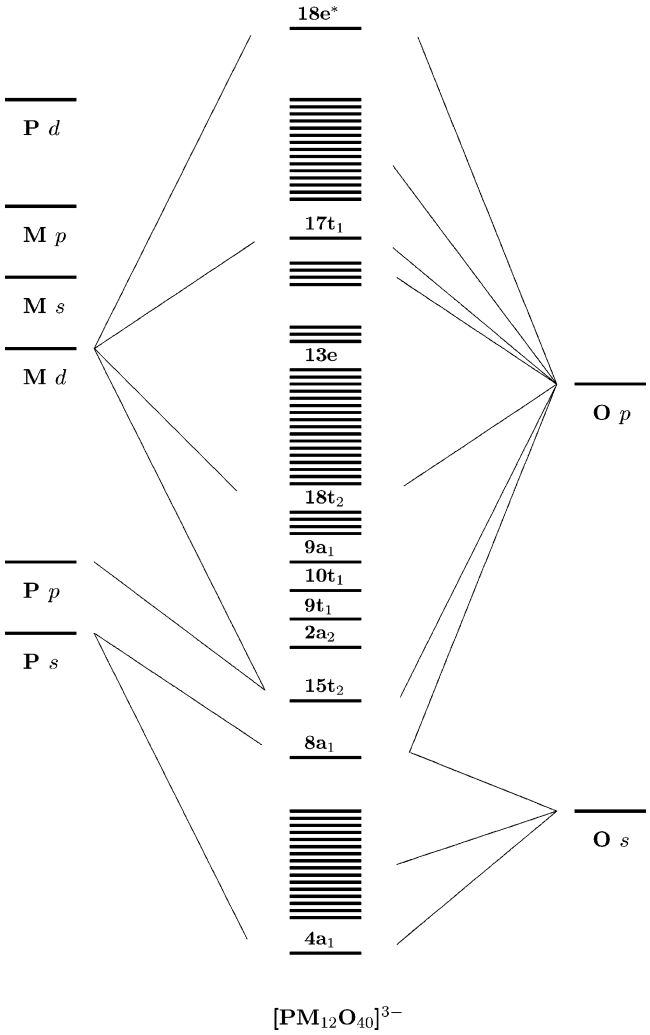

Figure 7. Qualitative molecular-orbital diagram showing predominant P, M, and O contributions to the valence levels of $[PM_{12}O_{40}]^{3-}$ anions.

Although the $[M_6O_6]$ structure occurs in several of the M−O bonding orbitals of the $[PM_{12}O_{40}]^{3-}$ clusters, it is also interesting to note that some of the levels comprising the predominantly M−O_{2c} group (for example, the 13e and $17t_1$ levels) include orbitals that can be described in terms of combinations of symmetry-adapted functions which do not contain a complete closed-loop structure.

A detailed analysis of the bonding energetics in a relatively large series of isopoly and heteropoly anions will be presented in a separate publication. In general, it can be concluded that the results obtained from the present calculations do not suggest that, in the $[TeM_6O_{24}]^{6-}$ and $[PM_{12}O_{40}]^{3-}$ species, the bridging bonds involved in closed loops should make a special contribution to the stability of these clusters.

Lowest-Unoccupied Orbitals. The lowest-unoccupied orbitals of the $[TeM_6O_{24}]^{6-}$ and $[PM_{12}O_{40}]^{3-}$ anions are shown, respectively, in Figures 12 and 13. These orbitals are equivalent in character and composition to the those of their respective model complexes, *cis*-$[MO_2Cl_4]^{2-}$ and $[MOCl_5]^{-}$.[39]

The calculations on $[TeM_6O_{24}]^{6-}$ anions predict that the lowest virtual level is the $9a_{2g}$ orbital. It can be described as a π-antibonding combination of d-type (d_{xy}, d_{xz}, d_{yz}) functions on the six metal atoms with p-type functions on (predominantly) the 12 terminal-oxygen atoms.

The calculations on the $[PM_{12}O_{40}]^{3-}$ anions indicate that the lowest-unoccupied orbitals correspond to the 18e level. These orbitals represent π-antibonding interactions between symmetry-adapted metal d_{xy}-like functions with (O_{2c}) bridging-oxygen p functions, and involve all (12) M and (24) O_{2c} sites.

The results for the $[PM_{12}O_{40}]^{3-}$ anions agree with the calculations reported by Poblet and co-workers[5,6] (who have employed a similar density-functional approach but different basis sets and relativistic treatment) but not with the topological analysis presented by King.[40] This yields a nondegenerate bonding orbital instead of the 18e level. As found for the $[M_6O_{19}]^{2-}$ species,[9] the discrepancy is likely to be the consequence of neglecting the antibonding interactions between M and O_{2c} atoms.[40]

Population Analysis. The results presented in this section are based on Mulliken and Mayer methodology. These methods are known to exhibit basis-set dependence, but (relative) Mulliken charges and Mayer bond indexes can nonetheless provide valuable chemical information for inorganic systems, if uniformity and consistency of the basis sets are maintained.[41] Furthermore, Mulliken analysis has been described as "not an arbitrary choice ... but consistent with the internal structure of the molecular-orbital formalism".[24]

The results from the application of population methods to the $[TeM_6O_{24}]^{6-}$ and $[PM_{12}O_{40}]^{3-}$ heteropolyanions are reported in the following three sections. Mulliken charges for all atoms are given in Table 2, and basis-function populations for Mo and W are included in Table 3. Mayer indexes for Te−O, P−O, and M−O bonds and valency indexes for the oxygen atoms are shown in Tables 4 and 5, respectively. Most results are largely similar to those obtained for isopolyanions.

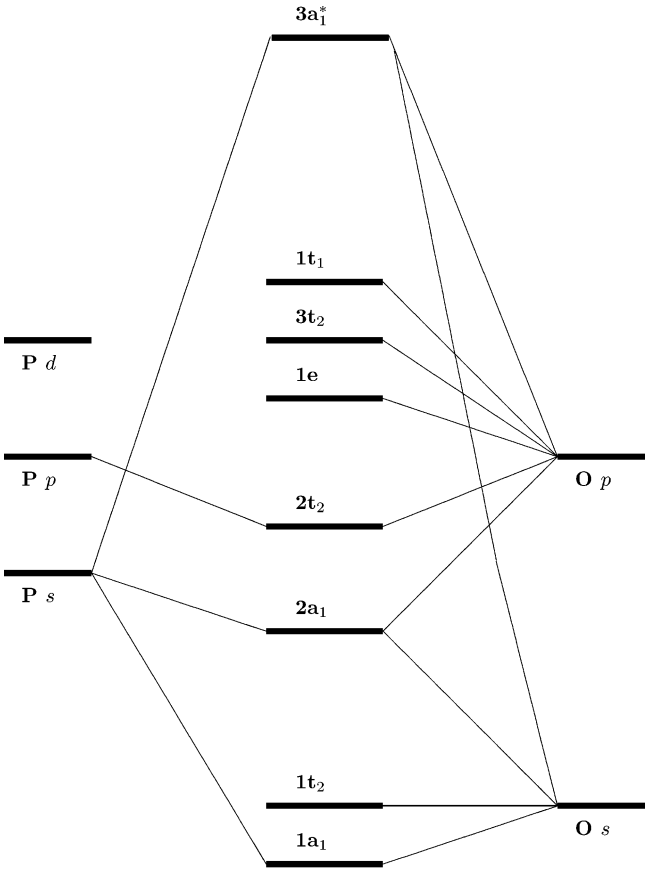

Figure 8. Qualitative molecular-orbital diagram showing predominant P and O contributions to the valence levels of $[PO_4]^{3-}$.

TABLE 2: Mulliken Charges for $[TeM_6O_{24}]^{6-}$ and $[PM_{12}O_{40}]^{3-}$ Anions

atom	$[TeMo_6O_{24}]^{6-}$	$[TeW_6O_{24}]^{6-}$
Te	+2.26	+2.29
M	+1.98	+2.14
O_t	−0.78	−0.84
O_{2c}	−0.88	−0.93
O_{3c}	−0.91	−0.92
atom	$[PMo_{12}O_{40}]^{3-}$	$[PW_{12}O_{40}]^{3-}$
P	+1.55	+1.73
M	+2.26	+2.34
O_t	−0.65	−0.69
O_{2c}	−0.85	−0.88
O_{4c}	−0.85	−0.83

TABLE 3: Populations of Mo and W Basis Functions (Given as Percentage per Individual Orbital) in $[TeM_6O_{24}]^{6-}$ and $[PM_{12}O_{40}]^{3-}$ Anions

molecule	s	p	d
$[TeMo_6O_{24}]^{6-}$	1.0	1.4	18.9
$[TeW_6O_{24}]^{6-}$	5.2	1.4	18.1
$[PMo_{12}O_{40}]^{3-}$	0.0	1.1	19.3
$[PW_{12}O_{40}]^{3-}$	3.1	1.3	18.6

Mulliken Data. The charges for both the metal (Mo, W) and heteroelement (Te, P) atoms are significantly smaller than the formal +5 or +6 oxidation states. The values for Mo and W correspond to electronic configurations that are close to d^4 and are somewhat higher for W (than Mo) because of the slightly higher s and lower d characters of the W basis-function

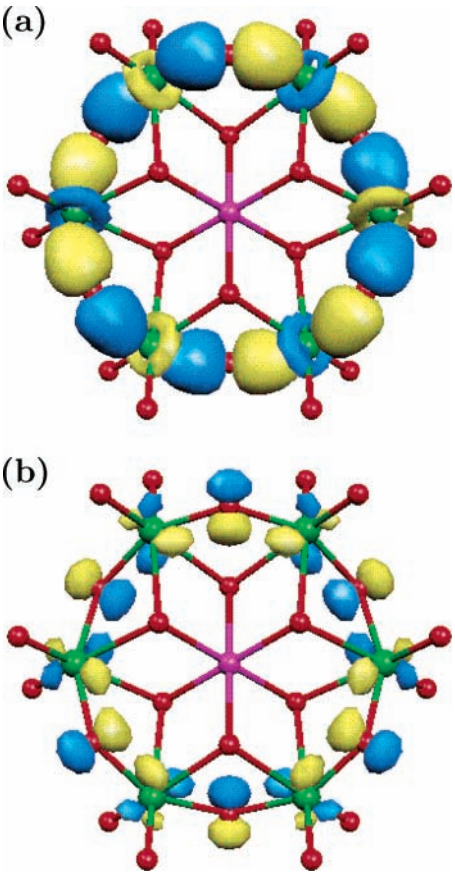

Figure 9. Spatial representation of (a) σ ($4a_{1u}$) and (b) π ($7a_{2u}$) $[M_6O_6]$ closed loops in $[TeM_6O_{24}]^{6-}$ anions.

TABLE 4: Mayer Indexes for $[TeM_6O_{24}]^{6-}$ and $[PM_{12}O_{40}]^{3-}$ Anions[a]

bond	$[TeMo_6O_{24}]^{6-}$		$[TeW_6O_{24}]^{6-}$	
Te−O_{3c}	0.78		0.77	
M−O_t	1.56	(1.45)	1.58	(1.46)
M−O_{2c}	0.73	(0.94)	0.73	(0.94)
M−O_{3c}	0.32	(0.42)	0.31	(0.38)
bond	$[PMo_{12}O_{40}]^{3-}$		$[PW_{12}O_{40}]^{3-}$	
P−O_{4c}	1.21		1.25	
M−O_t	1.68	(1.64)	1.74	(1.57)
M−O_{2c}	0.73	(1.01)	0.76	(0.99)
M−O_{4c}	0.13	(0.30)	0.13	(0.30)

[a] Results from classical bond-valence analysis are given in parentheses.

populations that are probably associated with relativistic effects.[42] The small values obtained for s and p contributions are in accordance with the results of the molecular-orbital analysis.

The oxygen values show a distribution of the negative charge over all types of sites. The lowest values correspond to the terminal sites, but these are nonetheless significantly charged. A somewhat different result from previous observations[9−12] is that, in both heteropoly species, the charges for O_{2c} and O_{3c} or O_{4c} atoms appear in general more similar than they do in (comparable) isopoly clusters.

Mayer Indexes. Mayer bond-order indexes are given in Table 4. Also included are the results obtained with a bond-valence model based on the following relationship[43]

$$\log s = \frac{(d_0 - d)}{B} \qquad (2)$$

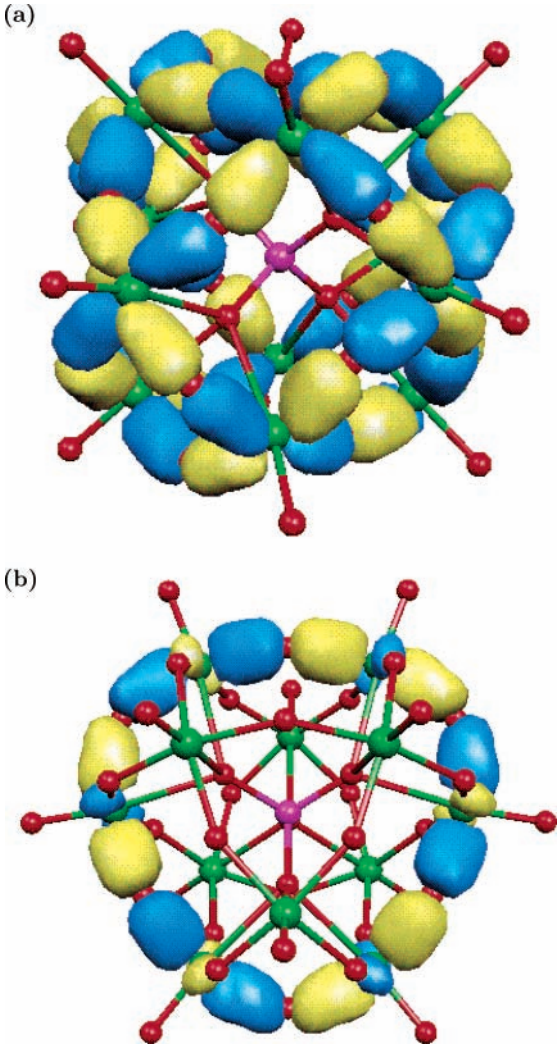

Figure 10. Spatial representation of σ ($2a_2$ orbital) closed loops in $[PM_{12}O_{40}]^{3-}$ anions: (a) three-dimensional structure and (b) $[M_6O_6]$ ring.

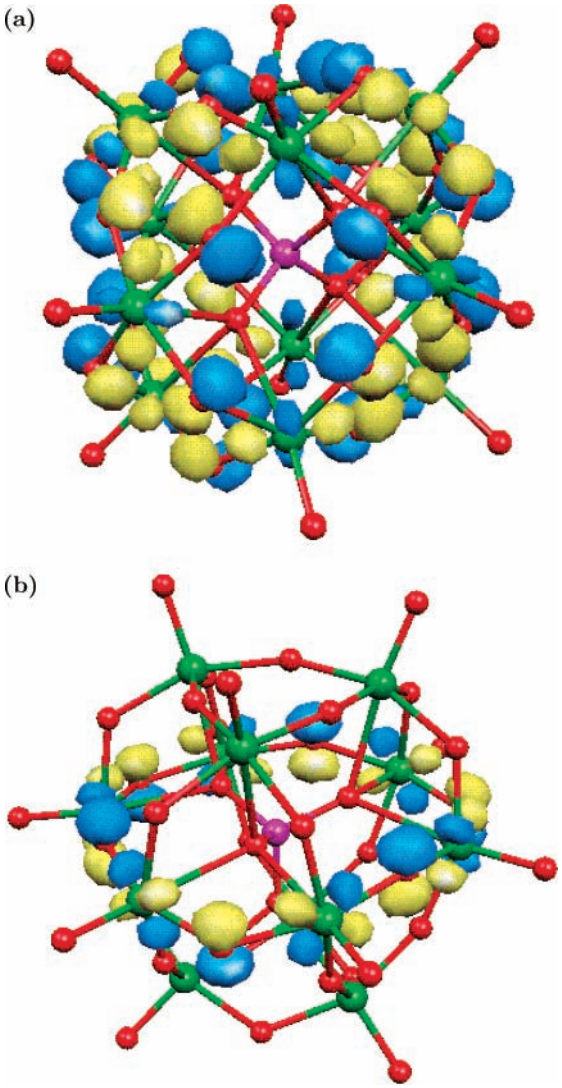

Figure 11. Spatial representation of π ($9a_1$ orbital) closed loops in $[PM_{12}O_{40}]^{3-}$ anions: (a) three-dimensional structure and (b) $[M_6O_6]$ ring.

TABLE 5: Covalency and Full-Valency Indexes for Oxygen Atoms in $[TeM_6O_{24}]^{6-}$ and $[PM_{12}O_{40}]^{3-}$ Anions

molecule	atom	covalency	full valency
$[TeMo_6O_{24}]^{6-}$	O_t	1.97	2.24
	O_{2c}	1.83	2.19
	O_{3c}	1.75	2.13
$[TeW_6O_{24}]^{6-}$	O_t	1.92	2.23
	O_{2c}	1.78	2.18
	O_{3c}	1.71	2.11
$[PMo_{12}O_{40}]^{3-}$	O_t	2.12	2.31
	O_{2c}	1.91	2.24
	O_{4c}	1.95	2.27
$[PW_{12}O_{40}]^{3-}$	O_t	2.09	2.30
	O_{2c}	1.86	2.22
	O_{4c}	1.95	2.26

where s is the bond valence, d_0 is the single-bond length, B defines the slope of the bond length-bond valence functions, and d is a calculated bond distance.

The calculated bond orders for metal−oxygen interactions in the heteropolyanions are in good agreement with the results obtained from application of eq 2. The deviations from the classical data and the general observations and trends are similar to those obtained for isopolyanions.

The $M-O_t$ indexes indicate appreciable degree of multiple bonding but, because of the significant charge on the terminal sites and the consequent ionic contributions, the Mayer values are rather smaller than the maximum possible covalencies. The analysis of the molecular orbitals associated with $M-O_{2c}$ interactions shows a multiple (σ/π) structure, but these orbitals are extensively delocalized and the $M-O_{2c}$ distances and indexes are more characteristic of approximately single bonds.

The O_{3c} and O_{4c} atoms lie in the trans configuration with respect to terminal bonds, and typically, their bonds to the metal sites exhibit considerably low orders. The $M-O_{4c}$ distances in $[PM_{12}O_{40}]^{3-}$ anions are among the longest calculated bond lengths, and have the lowest Mayer values within the set of polyoxoanions investigated in this and previous work. This result is probably the combined effect of the trans-to-oxo configuration and of the relatively strong P−O interactions.

In the $[TeM_6O_{24}]^{6-}$ anions, the $M-O_{3c}$ bonds are trans to two instead of three terminal oxo ligands, and the Te−O interactions seem to be somewhat weaker than a single bond. The $M-O_{3c}$ distances and indexes are then not as long and small as the (corresponding) $M-O_{4c}$ values in $[PM_{12}O_{40}]^{3-}$.

Oxygen Valency. The covalency and full-valency indexes shown in Table 5 suggest that, although the coordination environment and the nature of the M−O interactions are rather different, the various oxygen atoms in the $[TeM_6O_{24}]^{6-}$ and $[PM_{12}O_{40}]^{3-}$ anions have comparable overall bonding capacities.

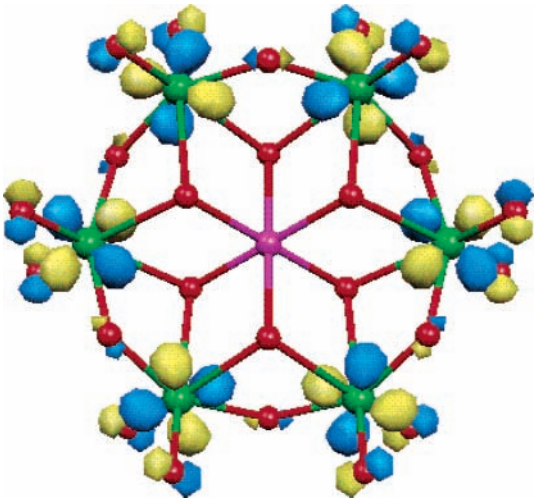

Figure 12. Spatial representation of the lowest-unoccupied ($9a_{2g}$) orbital of $[TeM_6O_{24}]^{6-}$ anions.

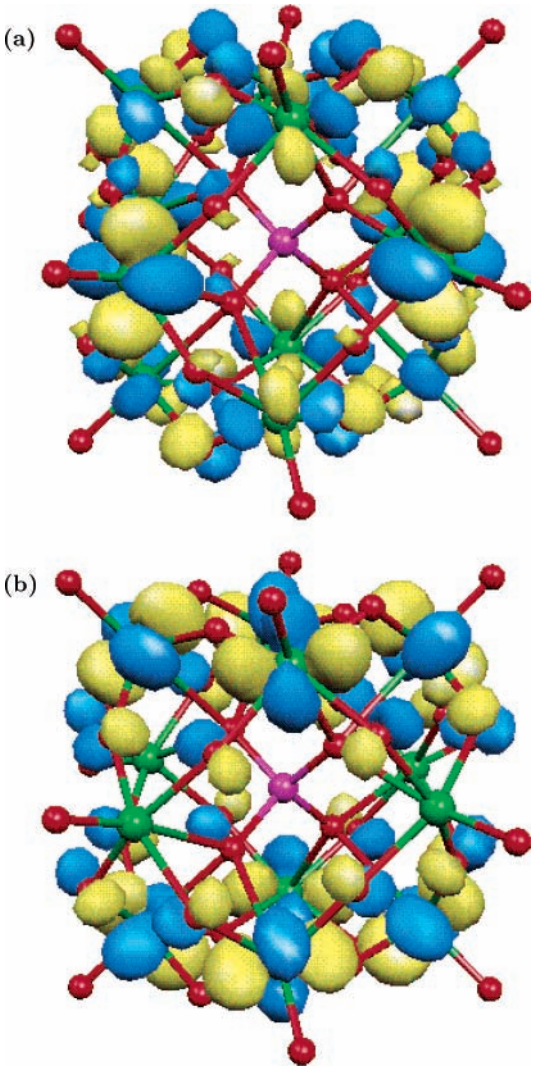

Figure 13. Spatial representation of the lowest-unoccupied (18e) orbitals of $[PM_{12}O_{40}]^{3-}$ anions.

This result is also observed in isopolyanions, but as noted in the Mulliken analysis, there is a difference, in this case in that the high-coordinate atoms, particularly the O_{4c} sites in $[PM_{12}O_{40}]^{3-}$, appear to be able to achieve a higher than typical relative covalency. The mechanism involved in counterbalancing the trans influence of the terminal bonds is a relatively strong interaction with the heteroatom. This seems to contribute to enhanced covalent character and lower relative charges for the trans-to-oxo atoms.

A similar observation can be made for the O_{3c} sites in the α isomer of the $[Mo_8O_{26}]^{4-}$ isopolyanion,[11] in which the formation of relatively strong $Mo_{4c}-O_{3c}$ bonds shows some resemblance to the effect of the $P-O_{4c}$ bonds in $[PM_{12}O_{40}]^{3-}$. (The Mo_{4c} atoms in α-$[Mo_8O_{26}]^{4-}$ have sometimes been treated as "hetero" sites[34] because the four-coordinate environment is not as commonly observed as the typical distorted octahedral configuration.)

TABLE 6: Fragment Analysis (in eV) for $[TeM_6O_{24}]^{6-}$ and $[PM_{12}O_{40}]^{3-}$ Anions[a]

molecule	ΔE_B	ΔE_O	ΔE_P	ΔE_E
$[TeMo_6O_{24}]^{6-}$	−52.67	−35.83	+51.54	−68.38
$[TeW_6O_{24}]^{6-}$	−55.48	−35.71	+53.57	−73.33
$[PMo_{12}O_{40}]^{3-}$	−22.35	−14.72	+33.20	−40.84
$[PW_{12}O_{40}]^{3-}$	−23.57	−15.56	+34.72	−42.72

[a] Results are based on eqs 4 and 5 and BP Calculations.

Fragment Analysis. Day and Klemperer[44] have considered that the structures of $[XM_{12}O_{40}]^{z-}$ anions could be described as a negatively charge $[XO_4]^{z-}$ unit encapsulated by a neutral $[M_{12}O_{36}]$ cage. This structural representation of Keggin anions has been supported by detailed calculations[6] on a relatively large series of Mo and W clusters. An equivalent description is, in principle, also possible for $[TeM_6O_{24}]^{6-}$ anions, namely, a $[TeO_6]^{6-}$ unit within an $[M_6O_{18}]$ cage.

The energetics of the interactions between the charged unit and the neutral cage can be evaluated using

$$E_B = E_O + E_P + E_E \tag{3}$$

and the following decomposition schemes for the heteropolyanions:

$$[M_6O_{18}]^{(0)} + [TeO_6]^{(6-)} = [TeM_6O_{24}]^{(6-)} \tag{4}$$

$$[M_{12}O_{36}]^{(0)} + [PO_4]^{(3-)} = [PM_{12}O_{40}]^{(3-)} \tag{5}$$

In eq 3, E_O, E_P, and E_E are respectively orbital-mixing, Pauli-repulsion, and electrostatic-interaction terms. Descriptions of the physical significance of these properties have been given by Landrum, Goldberg, and Hoffmann[45] and by Baerends and co-workers.[17,46] Both E_O and E_P represent orbital-interaction effects, but the former is stabilizing whereas the latter is destabilizing. The E_E contribution is primarily dominated by the nucleus-electron attractions, and therefore has a stabilizing influence.

The total molecular bonding energy relative to the fragments is given by

$$\Delta E_B = \Delta E_O + \Delta E_P + \Delta E_E \tag{6}$$

The results are shown in Table 6. The stabilization of the anionic fragments inside the cages is due to both orbital-mixing and electrostatic effects, with the relative contributions being 0.34/0.66 and 0.27/0.73 ($\Delta E_O/\Delta E_E$) for $[TeM_6O_{24}]^{6-}$ and $[PM_{12}O_{40}]^{3-}$, respectively. The magnitude of all energy terms is greater in the Anderson than α-Keggin structures, in accordance with the respective M−O parameters suggesting that the $M-O_{3c}$ interactions in the former should be stronger than the $M-O_{4c}$ interactions in the latter.

Poblet and co-workers[6] have considered that, although orbital-mixing effects are significant, in the Keggin systems most of

TABLE 7: Mayer Indexes for $[TeO_6]^{6-}$ and $[PO_4]^{3-}$ Ions and $[M_6O_{18}]$ and $[M_{12}O_{36}]$ Cages

molecule	bond	index
$[TeO_6]^{6-}$	Te−O	1.14
$[Mo_6O_{18}]$	Mo−O_t	1.82
	Mo−O_{2c}	0.76
$[W_6O_{18}]$	W−O_t	1.87
	W−O_{2c}	0.79
$[PO_4]^{3-}$	P−O	1.70
$[Mo_{12}O_{36}]$	Mo−O_t	1.79
	Mo−O_{2c}	0.75
$[W_{12}O_{36}]$	W−O_t	1.84
	W−O_{2c}	0.78

this contribution arises from the polarization of the $[M_{12}O_{36}]$ cage by the $[PO_4]^{3-}$ fragment. These authors have concluded that there is only limited covalent character in these ion−cage interactions and that the structural model proposed by Day and Kemplerer can, therefore, be considered satisfactory.

The molecular-orbital analysis of $[TeM_6O_{24}]^{6-}$ and $[PM_{12}O_{40}]^{3-}$ indicates that the Te−O and P−O bonding structures display minor differences whether the ionic fragments are considered separately or as part of the clusters. However, some orbital mixing between the internal oxygen (O_{3c} or O_{4c}) sites and the metal atoms is observed. The Mayer analysis suggests that the covalent effects associated with these internal M−O bonds may be significant despite being (relatively) small. Table 7 contains calculated indexes for the Te−O and P−O bonds in the $[TeO_6]^{6-}$ and $[PO_4]^{3-}$ ions and for the M−O bonds in the $[M_6O_{18}]$ and $[M_{12}O_{36}]$ cages.

The Mayer index for P−O interactions decreases significantly in $[PM_{12}O_{40}]^{3-}$ (with respect to $[PO_4]^{3-}$), but the combined M−O_{4c} bond order is considerably smaller than the P−O_{4c} bond order. It is nevertheless interesting to note that, although the changes in the indexes for M−O_t and Mo−O_{2c} interactions are comparatively less important, the bond-order sums for Mo and W atoms are only marginally different in the isolated cages and the polyanions, as some covalent character appears to be transferred primarily from the M−O_t bonds into the M−O_{4c} bonds (the O_t and O_{4c} atoms being trans connected along an approximate C_4 axis in the individual $[MO_6]$ units).

The Mayer index for Te−O interactions is significantly smaller in $[TeM_6O_{24}]^{6-}$ (with respect to $[TeO_6]^{6-}$), and its value is actually close to the combined M−O_{3c} bond order. Also, although the M−O_t indexes are somewhat higher in the isolated cages than in the polyanions, the Mo and W bond-order sums are (largely) conserved, apparently because of a relatively important transfer of covalent character between the trans-connected M−O_t and M−O_{3c} bonds (the Mo−O_{2c} indexes remaining mostly unchanged). In general, the magnitude of the covalent effects associated with the internal M−O bonds suggests that the ion-cage model does not seem appropriate in this case.

Conclusion

The molecular and electronic structures of (Anderson) $[TeM_6O_{24}]^{6-}$ and (α-Keggin) $[PM_{12}O_{40}]^{3-}$ heteropolyanions have been calculated by density-functional methods and analyzed with a combination of molecular-orbital, population, and fragment-decomposition approaches. In general, the computational bond parameters compare well with experimental and classical bond-valence results, as previously observed for isopolyanions.

The molecular-orbital and population analyses have indicated that the M−O interactions are largely of M*d*−O*p* character, and can be characterized as (fractional) multiple terminal bonds, approximately single bridging (M−O_{2c}) bonds, and low-order internal (M−O_{3c} and M−O_{4c}) bonds, in accord with structural and bond-valence data. Multicentered bonds of σ and π nature are formed between the metal sites and the bridging-oxygen atoms, and these M−O_{2c} orbital interactions can be described in terms of the $[M_6O_6]$ closed loops proposed by Nomiya and Miwa.

The bonding between the internal oxygen sites and the Te or P heteroatoms has been found to occur through interactions involving the s and p orbitals of the Te or P atoms and of the O atoms. The comparison of the electronic structures of the actual clusters with those of model $[TeO_6]^{6-}$ and $[PO_4]^{3-}$ species has indicated that the molecular-orbital structure of the bonding to the heteroatom is not significantly affected by the surrounding metal−oxygen cage. Nevertheless, the calculations have suggested some degree of covalent character in the interactions between Te−O or P−O bonds and the internal M−O bonds. This appears to be a phenomenon of small magnitude in $[PM_{12}O_{40}]^{3-}$ anions, but it has been found to be more significant in $[TeM_6O_{24}]^{6-}$ anions.

Valency results have indicated that, as in the isopolyanions, the overall bonding capacities of the various oxygen atoms are relatively similar despite the differences in the coordination environments and individual bond properties. The internal sites are involved in comparatively strong interactions with the heteroatom, which appear to contribute to compensating for the relative weakness of their (individual) bonds to the metal atoms.

Acknowledgment. The authors thank EPSRC, the Cambridge Overseas Trust, Selwyn College (Cambridge), and the University of Hull for financial support and the Computational Chemistry Working Party for access to computational facilities in the Rutherford Appleton Laboratory.

References and Notes

(1) Pope, M. T. *Heteropoly and Isopoly Oxometalates*; Springer-Verlag: Heidelberg, 1983.
(2) Pope, M. T.; Müller, A. *Angew. Chem. Int. Ed. Eng.* **1991**, *30*, 34.
(3) Pope, M. T.; Müller, A.; editors. *Polyoxometalates: from Platonic Solids to Anti-retroviral Activity*; Kluwer: Dordrecht, The Netherlands, 1994.
(4) Baker, L. C. W.; Glick, D. C. *Chem. Rev.* **1998**, *98*, 3.
(5) Maestre, J. M.; López, X.; Bo, C.; Poblet, J. M.; Casañ-Pastor, N. *J. Am. Chem. Soc.* **2001**, *123*, 3749.
(6) López, X.; Maestre, J. M.; Bo, C.; Poblet, J. M. *J. Am. Chem. Soc.* **2001**, *123*, 9571.
(7) Bridgeman, A. J.; Cavigliasso, G. *Polyhedron* **2001**, *20*, 3101.
(8) Bridgeman, A. J.; Cavigliasso, G. *Polyhedron* **2002**, *21*, 2201.
(9) Bridgeman, A. J.; Cavigliasso, G. *Inorg. Chem.* **2002**, *41*, 1761.
(10) Bridgeman, A. J.; Cavigliasso, G. *J. Chem. Soc., Dalton Trans.* **2002**, 2244.
(11) Bridgeman, A. J.; Cavigliasso, G. *Inorg. Chem.* **2002**, *41*, 3500.
(12) Bridgeman, A. J.; Cavigliasso, G. *J. Phys. Chem. A* **2002**, *106*, 6114.
(13) Baerends, E. J.; Ellis, D. E.; Ros, P. *Chem. Phys.* **1973**, *2*, 41.
(14) Versluis, L.; Ziegler, T. *J. Chem. Phys.* **1988**, *88*, 322.
(15) te Velde, G.; Baerends, E. J. *J. Comput. Phys.* **1992**, *99*, 84.
(16) Fonseca Guerra, G.; Snijders, J. G.; te Velde, G.; Baerends, E. J. *Theor. Chem. Acc.* **1998**, *99*, 391.
(17) te Velde, G.; Bickelhaupt, F. M.; Baerends, E. J.; Fonseca Guerra, C.; van Gisbergen, S. J. A.; Snijders, J. G.; Ziegler, T. *J. Comput. Chem.* **2001**, *22*, 931.
(18) Vosko, S. H.; Wilk, L.; Nusair, M. *Can. J. Phys.* **1980**, *58*, 1200.
(19) Kohn, W.; Sham, L. J. *Phys. Rev.* **1965**, *140*, A1133.
(20) Becke, A. D. *Phys. Rev. A* **1988**, *38*, 3098.
(21) Perdew, J. P. *Phys. Rev. B* **1986**, *33*, 8822.
(22) Bridgeman, A. J.; Cavigliasso, G. *Polyhedron* **2001**, *20*, 2269.
(23) Bridgeman, A. J.; Cavigliasso, G. *J. Phys. Chem. A* **2001**, *105*, 7111.
(24) Mayer, I. *Chem. Phys. Lett.* **1983**, *97*, 270.
(25) Mayer, I. *Int. J. Quantum Chem.* **1984**, *26*, 151.

(26) Evarestov, R. A.; Veryazov, V. A. *Theor. Chim. Acta* **1991**, *81*, 95.
(27) MAYER. Bridgeman, A. J.; Empson, C. J. University of Hull, U.K., 2002.
(28) MOLEKEL: An Interactive Molecular Graphics Tool; Portmann S.; Lüthi, H. P. *CHIMIA* **2000**, 54, 766.
(29) Robl, C.; Frost, M. *Z. Naturforsch.* **1993**, *48b*, 404.
(30) Lorenzo-Luis, P. A.; Gili, P.; Sánchez, A.; Rodriguez-Castellón, E.; Jiménez-Jiménez, J.; Ruiz-Pérez, C.; Solans, X. *Trans. Metal Chem.* **1999**, *24*, 686.
(31) Ugalde, M.; Gutierrez-Zorrilla, J. M.; Vitoria, P.; Luque, A.; Wery, A. S. J.; Roman, P. *Chem. Mater.* **1997**, *9*, 2869.
(32) Bi, L. H.; Wang, E. B.; Xu, L.; Huang, R. D. *Inorg. Chim. Acta* **2000**, *305*, 163.
(33) Nolan, A. L.; Allen, C. C.; Burns, R. C.; Craig, D. C.; Lawrance, G. A. *Aust. J. Chem.* **2000**, *53*, 59.
(34) Nomiya, K.; Miwa, M. *Polyhedron* **1984**, *3*, 341.
(35) Nomiya, K.; Miwa, M. *Polyhedron* **1985**, *4*, 89.
(36) Nomiya, K.; Miwa, M. *Polyhedron* **1985**, *4*, 675.
(37) Nomiya, K.; Miwa, M. *Polyhedron* **1985**, *4*, 1407.
(38) Nomiya, K. *Polyhedron* **1987**, *6*, 309.
(39) Bridgeman, A. J.; Cavigliasso, G., *J. Chem. Soc., Dalton Trans.* **2001**, 3556.
(40) King, R. B. *Inorg. Chem.* **1991**, *30*, 4437.
(41) Bridgeman, A. J.; Cavigliasso, G., Ireland, L. R.; Rothery, J. *J. Chem. Soc., Dalton Trans.* **2001**, 2095.
(42) Kaltsoyannis, N. *J. Chem. Soc., Dalton Trans.* **1997**, 1.
(43) Tytko, K. H.; Mehmke, J.; Fischer, S. *Struct. Bonding* **1999**, *93*, 129.
(44) Day, V. W.; Klemperer, W. G. *Science* **1985**, *228*, 533.
(45) Landrum, G. A.; Goldberg, N.; Hoffmann, R. *J. Chem. Soc., Dalton Trans.* **1997**, 3605.
(46) Bickelhaupt, F. M.; Baerends, E. J. *Rev. Comput. Chem.* **2000**, *15*, 1.